Egyptian Journal of Chemistry

http://ejchem.journals.ekb.eg/

Synthesis, spectroscopic, DFT and docking studies, Molecularstructure of new Schiff base metal complexes

Ehab M. Zayed[a]*, Gehad G. Mohamed[b]

[a] *Green Chemistry Department, National Research Centre, Dokki, 12622 Giza, Egypt*

[b] *Chemistry Department, Faculty of Science, Cairo University, 12613 Giza, Egypt*

Abstract

A Schiff base ligand (H_2L) and its complexes have been synthesized and characterized by analytical tools, spectral (IR and ^1H NMR), molar conductivity and magnetic moment measurements. The thermal analysis (TG) technique is studied within the temperature range from room temperature to 1000 ^0C. The IR spectra pointed out that the ligand (H_2L) coordinated to the metal ions through two nitrogen and four oxygen atoms in a neutral mode. The structural formula of the synthesized Schiff base ligand was optimized using Gaussian09 program where the energy gaps and other important theoretical parameters were calculated applying the DFT/B3LYP method. *In vitro* biological activities of the Schiff base ligand (H_2L) and its metal complexes were screened against Gram(+) bacteria (*Bacillis subtilis* and *Staphylococcus aureus*) and Gram(-) bacteria (*Escherichia coli* and *Pseudomonas aeruginosa*) using agar diffusion method. The results illustrated that the synthesized complexes are biologically active than the Schiff base ligand. Molecular docking study was carried out between the Schiff base ligand and crystal structure of *Escherichia Coli*, crystal structure of *Staphylococcus Aureus*, crystal structure of *Bacillus subtilis* and crystal structure of *P. aeruginosa*.

Keywords: Schiff base complexes, spectroscopic and thermal analyses, antimicrobial activity, anticancer activity, Molecular docking

1. Introduction

Many cyclic peptides used in clinic, and the most of them originate from the natural cyclic peptides [1]. As several features make cyclic peptides attractive lead compounds for drug development as well as nice tools for biochemical research, scientists made diverse efforts to develop biologically active cyclic peptide compounds [2-6]. Thus, synthetic peptides, as initial biological leads, allow rapid identification of the molecular structural requirements of active drug modulators. Many natural, as well as, synthetic peptides having interesting biological activities are, progressively, reported [7-9]. However, synthetically, the conversion of the active linear peptides into their cyclic congeners, or the corresponding peptidomimetics, can be formed by linking one end of the peptide and the other with an amide bond between amino and carboxyl termini N-to-C (or head-to-tail), constitute a major class of important anticancer therapeutic agents, as well as antimicrobial, antibacterial activity, and anti-inflammatory agents [9-11] Macrocyclic peptide ligands which have additional donor atoms appended to the ring has attracted considerable interest due to their capacity to bind and transport metal ions. There is a continued interest in the synthesis of macrocyclic complexes [11, 12] because of their potential applications in fundamental and applied sciences [13, 14] and a huge impact on cancer chemotherapy due to their anticancer activity and importance in the area of coordination chemistry [15, 16] Cyclic peptides also exhibit specificity in the binding of certainmetal ions. Studies with cyclopeptides like vasopressin or oxytocinhave shown that theseapparently naturally metal-free substances effectively bind metal ions [17, 18]. The cyclic peptides have been obtained by peptide bond formation between the N-terminal amine and the C-terminal carboxylate groups of

*Corresponding author e-mail: ehab_zayed2002@yahoo.com.
Receive Date: 05 July 2021, Revise Date: 17 July 2021, Accept Date: 27 July 2021
DOI: 10.21608/EJCHEM.2021.83871.4116

linear precursors. The impact of the N-terminal amino group (alsoknown as the metal ion anchoring group) on complex formation is observed also in His-containing peptides [19, 20].

In this article, Cd(II), Mn(II) and Zn(II) complexes of a newly cyclopeptide ligand were synthesized and characterized using different analytical and physicochemical techniques. Their antibacterial activity against a number of bacteria organisms were screened. Molecular docking studies have been performed against crystal structure of 3t88-Escherichia Coli, crystal structure of 3ty7-Staphylococcus Aureus, crystal structure 5h67-Bacillus subtilis and crystal structure 5i39-P. aeruginosa to gain an insight into the possible mechanistic action in search of good potent antitubercular candidates.

2. Experimental

2. l. Materials and reagents:

All chemicals used were of the analytical reagent grade (AR), and of highest purity available. The chemicals used involved N1,N3-diphenethyl-isophthalamide and 2,6-bis(2-formamido-3-phenyl-propanamido)hexanoate, which were supplied from Sigma-Aldrich. $MnCl_2.2H_2O$ (BDH), $ZnCl_2.2H_2O$ (BDH) and $CdCl_2.2H_2O$ (BDH) (Prolabo) were used. Organic solvents were spectroscopic pure from BDH included ethanol, diethyl ether and dimethylformamide. Hydrogen peroxide, sodium chloride, sodium carbonate, glacial acetic acid and sodium hydroxide (A.R.) were used.

2.2. Solutions

For molar conductivity measurement, $1x10^{-3}$ M stock solutions of the Schiff base ligand and metal complexes were prepared using dimethylformamide solvent. For measuring UV–Vis absorption spectra, $1x10^{-4}$ M solutions of the Schiff base ligand and metal complexes were prepared by accurate dilution from the previous prepared stock solutions. For the preparation of RPMI-l640 medium, sodium bicarbonate (Sigma Chemical Co., St. Louis, Mo, USA) was used. In normal saline, 0.05% isotonic Trypan blue solution (Sigma Chemical Co., St. Louis, Mo, USA) was prepared and used to count viability. Sigma Chemical Co., St. Louis, Mo, USA supplied 10 percent Fetal Bovine Serum (FBS) (heat inactivated at 56 ºC for 30 min), l00 units/ml Penicillin and 2 mg/ml Streptomycin and was used prior to use for RPMI-1640 medium supplementation. For cell harvesting, 0.025 percent (w/v) Trypsin (Sigma Chemical Co., St. Louis, Mo, USA) was used. For the dissolution of the unbound SRB dye, 1% (v/v) Acetic acid (Sigma Chemical Co., St. Louis, Mo, USA) was used. As a protein dye, 0.4% of Sulphorhodamine-B (SRB) (Sigma Chemical Co., St. Louis, Mo, USA) dissolved in 1% acetic acid was used. A stock solution (TCA, 50%, Sigma Chemical Co., St. Louis, Mo, USA) of trichloroacetic acid has been prepared and processed. To yield a final concentration of 10 percent used for protein precipitation, 50 µL of the stock was applied to 200 µl RPMI-l640 medium/well. Isopropanol 100 percent and ethanol 70 percent were used. For SRB dye solubilization, Tris base 10 mM (pH 10.5) was used. In 1000 ml of distilled water, 121.1 g of tris base was dissolved and pH was modified by HCl acid (2 M).

2.3. Instrumentations

Carbon, hydrogen and nitrogen microanalyses were performed using the CHNS-932 (LECO) Vario Elemental Analyzer at the Microanalytical Center, Cairo University, Egypt. FT-IR spectra were registered as KBr discs. At room temperature, electronic spectra were registered as solutions in ethanol on a Shimadzu 3101pc spectrophotometer. As a solution in DMSO-d_6, ^{1}H NMR spectra were recorded at room temperature on a 500 MHz Varian-Oxford Mercury using TMS as an internal standard. Using the Jenway 4010 conductivity meter, the molar conductivity of 10-3 M solid complex solutions in DMF was calculated. The absorption spectra were recorded for 1×10^{-4} M solutions of the free Schiff base ligand and metal complexes. The spectra were scanned within the wavelength range from 200 to 700 nm. Thermogravimetric analyses (TG and DTG) of solid complexes were performed using the Shimadzu TG-50H thermal analyzer from room temperature to 1000 ºC. A (Quanta FEG250) SEM, National Research Center, Egypt) recorded a scanning electron microscope (SEM) image of thecomplexes. Using the MS-5988 GS-MS Hewlett-Packard instrument at the Microanalytical Center, National Center for Research, Egypt, mass spectra were recorded by the EI technique at 70 eV. The

antimicrobial activities were carried out at the University of Cairo Microanalytical Center.

2.4. Synthesis of Schiff base ligand

The Schiff base ligand was synthesized as previously described [21]

2.5. Synthesis of metal complexes

By mixing equal amounts (0.347 mmol) of hotethanol solution of the Schiff base ligand with the same metal chloride ratio, the Mn(II), Cd(II) and Zn(II) complexes were prepared (lM : lL molar ratio). For three hours, the mixture was refluxed. Through filtration, the resulting precipitates were collected and washed several times with hot ethanol until the filtrates were clear in order to provide 85, 85 and 88 percent yield of Mn(II), Cd(II) and Zn(II) complexes, respectively. The solid complexes then dried in desiccator over anhydrous calcium chloride.

Cyclo - (isophthaloyl) - [L – Phe – L -Phe] –Lys Cd(II) chloride $[Cd(H_2L)].Cl_2$; Yield 85%; m.p. 277 °C; Green solid. Anal. Calc. for $C_{50}H_{52}Cl_2CdN_6O_8$ (%): C, 55.38; H, 5.21; N, 7.75, Cl, 6.56; M, 10.37. Found (%):C, 55.73; H, 5.26; N, 7.80, Cl, 6.58; M, 10.35. FT-IR (KBr, ν, cm^{-1}) 3409 (COOH), 3065 (NH stretching), 2930 (CH, aromatic), 2090 (CH aliphatic), 1648 (C=O, acid), 1250 and 1089 (C=O, amide I and II, respectively), 526 (M─O), 422 (M─N). μ_{eff} (BM) diamagnetic; Λ_m (Ω^{-1} mol^{-1} cm^2) 103.5. UV-Vis (λ_{max}, nm): 270 (π–π* of aromatic rings).

Cyclo - (isophthaloyl) - [L – Phe – L -Phe] –Lys Zn(II) chloride $[Zn(H_2L)].Cl_2$; Yield 88%; m.p. 280 °C; Dark Blue solid. Anal. Calc. for $C_{50}H_{52}Cl_2ZnN_6O_8$ (%): C, 57.89; H, 5.44; N, 8.10, Cl, 6.84; M, 6.30. Found (%): C, 57.93; H, 5.48; N, 8.15, Cl, 6.88; M, 9.35. FT-IR (KBr, ν, cm^{-1}) 3334 (COOH), 3050 (NH stretching), 2925 (CH, aromatic), 2092 (CH aliphatic), 1640 (C=O, acid), 1251 and 1091 (C=O, amide I and II, respectively), 530 (M─O), 432 (M─N). μ_{eff} (BM) diamagnetic; Λ_m (Ω^{-1} mol^{-1} cm^2) 95. UV-Vis (λ_{max}, nm): 270 (π–π* of aromatic rings).

Cyclo - (isophthaloyl) - [L – Phe – L -Phe] –Lys Mn(II) chloride $[Mn(H_2L)].Cl_2$; Yield 90%; m.p. 258 °C; yellowish brown solid. Anal. Calc. for $C_{50}H_{52}Cl_2MnN_6O_8$ (%): C, 58.48; H, 5.50; N, 8.18, Cl, 6.91; M, 5.4.23. Found (%): C, 58.53; H, 5.55; N, 8.23, Cl, 6.95; M, 5.35. FT-IR (KBr, ν, cm^{-1}) 3400 (COOH), 3066 (NH stretching), 2934 (CH, aromatic), 2093 (CH aliphatic), 1646 (C=O, acid), 1290 and 1094 (C=O, amide I and II, respectively), 530 (M─O), 425 (M─N). μ_{eff} (BM) 5.17; Λ_m (Ω^{-1} mol^{-1} cm^2) 97. UV-Vis (λ_{max}, nm): 270 (π–π* of aromatic rings).

2.6. Spectrophotometric studies

The absorption spectra were recorded for 1×10^{-4} M solutions of the free Schiff base ligand and metal complexes. The spectra were scanned within the wavelength range from 200 to 700 nm.

2.7. Molecular docking

AutoDock 4.2 and docking computations applying Gasteiger partial charges added to ligand

(designed drug) atoms were used as previously described [22, 23]

2.8. Biological Activity

The diffusion agar method was used to test the biological activity of the Schiff base ligand and complexes and the details of the method were previously described. The antibacterial activities were calculated as a mean of three replicates and the MIC_{50} was determined [24-28]

2.9. Computational methodology:

The optimized structural geometry of the Schiff base ligand was determined using the DFT/B3LYP method with different base sets using Gaussian09 software [29] and the significant bond lengths, oscillator strengths, excitation energies and effective charges for coordinating groups in optimized structures were deduced.

2.10. Molecular Docking

AutoDock 4.2 and docking computations applying Gasteiger partial charges added to ligand (designed drug) atoms were used as described previously [1, 30-32]

3. Results and discussion

The synthesized Schiff base ligand (H_2L) was characterized using elemental analysis (C, H, N),

infrared spectral studies (IR), ^{1}H and ^{13}C NMR, mass spectra and thermal analysis (TG and DTG) as previously described.The optimized geometrical structure of the Schiff base ligand using molecular modelling with the Gaussian09 program was given in Figure (1) and Figure (2) [33, 34] and the data obtained were given in the previous study.

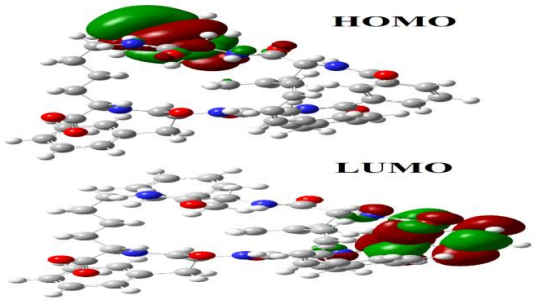

Figure 1. HOMO-LUMO of ligand

3.1. Characterization of metal complexes

The physical, analytical and spectroscopic data of the complexes were summarized in the experimental part (Table (1). They are air stable and soluble in DMF and DMSO solvents but insoluble in MeOH, EtOH, acetone, CCl_4 and benzene. There is satisfactory agreement between the calculated and found percentages elemental analyses data which confirmed the formation of complexes in 1 M : 1 L ratio [35-40]

Table 1. Elemental and physical data of Schiff base metal complexes.

Complex	Colour (% yield)	M.P (°C)	% Calcd. (Found)					μ_{eff} (B.M)	Λ_m $\Omega^{-1}mol^{-1}cm^2$
			C	H	N	Cl	M		
$[Cd(H_2L)].Cl_2$	Green (85)	277	55.43 (55.38)	5.26 (5.21)	7.80 (7.75)	6.58 (6.54)	10.37 (10.31)	Diam	72
$[Zn(H_2L)].Cl_2$	Dark Blue (88)	280	57.93 (57.89)	5.48 (5.44)	8.15 (8.10)	6.88 (6.84)	6.30 (6.24)	Diam	103
$[Mn(H_2L)].Cl_2$	Yellowish brown (85)	258	58.53 (58.48)	5.55 (5.50)	8.23 (8.18)	6.95 (6.91)	5.35 (5.29)	5.17	122

3.2. IR spectral studies

The IR spectra of the free Schiff base ligand and metal complexes were carried out in the range of 4000-400 cm^{-1}, and the most effective bands are given in the experimental part. The sharp stretching vibration bands observed at 3030-3066 cm^{-1} (3065 cm^{-1} in the free ligand) indicating that the ligand coordinates to metal ions via amine moiety. The complexes exhibited bands in the range of 1250-1294 and 1072-1098 cm^{-1} in comparison with the free ligand at 1258 and 1110 cm^{-1} which attributed to the amide (C=ONH) group. This shift in band position confirmed that the complexation reaction occurred through formation of coordinate bond with nitrogen oxygen atoms of the Schiff base ligand [41]. The medium and week bands found in the spectra of thecomplexes in the range of 515-541 cm^{-1} and 420-432 cm^{-1} can assigned to ν(M-O) and ν(M-N) stretching vibrations, respectively [42-46]. According to the above data, it can conclude that the Schiff base ligand behaved as neutral hexadentate ligand and coordinated to the metal ions via the tow amide nitrogen atoms and the four carbonyl oxygen atoms of the amide group.

3.3. ^{1}H-NMR spectra:

The ^{1}H-NMR spectrum of the Schiff base ligand was compared with that of Zn(II) and Cd(II) complexes and the data obtained revealed that the signals still appeared at the same position as the ligand but enhancement decrease which support the coordination of Schiff base ligand to metal ions with protonated amide group.[47]

3.4. Molar conductivity measurements

In order to detect if the counter ions either outside or inside the coordination sphere, the conductivity measurements must be measured where it can indicate the degree of ionization of the prepared complexes. The molar conductivity of 1×10^{-3} M solutions of the prepared metal complexes in DMF solvent was measured and was found to be were 103.5, 95 and 97 $\Omega^{-1}cm^2mol^{-1}$ for Cd(II), Zn(II) and Mn(II) complexes, respectively. Thesedata supported the electrolytic nature of the complexes.

3.5. Electronic spectra and magnetic moment measurements

It is possible to draw up the electronic transitions and detect the geometry with the help of magnetic moments of most metal ions [48]. The diffused reflectance spectrum of the Mn(II) complex pointed out three bands at 14,656, 19,478 and 23,945 cm^{-1} which are assigned to $^4A_{1g} \rightarrow {}^6A_{1g}$, $^4T_{2g}$ (G)$\rightarrow {}^6A_{1g}$ and $^4T_{1g}$ (D)$\rightarrow {}^6A_{1g}$ transitions, respectively. It has μ_{eff} value of 5.17 B.M. which confirmed octahedral geometry of the Mn(II) complex [49]. Zn(II) and Cd(II) complexes are diamagnetic and according to their empirical formula, they have octahedral geometry.

3.6. Mass Spectral studies

The mass of spectra of the for $[Cd(H_2L)].Cl_2$, $[Zn(H_2L)].Cl_2$ and $[Mn(H_2L)].Cl_2$ complexes showed molecular ion peaks at m/z 1048.25, 1034.27 and 1025.28 amu, respectively. Their spectra of the complexes showed also molecular ion (m/z) peaks at 854 amu corresponding to the Schiff base ligand which further support complex formation.

3.7. UV-Visible spectra of the ligand and its metal complexes

The UV-visible spectrum of the Schiff base ligand showed sharp peak at 276 nm that corresponding to π-π* transitions within the phenyl and azomethine groups [50-55]. This peak was found in the complexes at270 nm indicated the participation of azomethine group in coordination.

3.8. Thermal analysis studies (TG and DTG):

The TG thermogram of [Cd(H2L)]Cl2 complex showed five decomposition steps. The first decomposition step accompanied by loss of 2HCl and CH4 molecules in the temperature range of 60-200 ºC with an estimated weight loss of 11.07% (calcd. 11.23%). The second decomposition step accompanied by loss of 3NO and C9H9N molecules in the temperature range of 200-450 oC with an estimated weight loss of 20.75% (calcd. 20.25%). The third and fourth steps of decomposition showed loss of N_2O, $C_{20}H_{12}$ and $C_{13}H_{12}O_2$ molecules at 450-600 ºC and 600-800 ºC with an estimated weight loss of 28.22% (calcd. 28.41%) and 18.45% (calcd. 18.75). The last step accompanied by loss of $C_7H_{13}O$ molecules in the temperature range of 800-1000 ºC with an estimated weight loss of 10.42% (calcd. 9.56%). Thereafter, the percentage of the residue corresponds to cadmium oxide contaminated with carbon and the total approximate weight loss was found to be 88.90% (calcd. 88.20%).

The TG thermogram of $[Zn(H_2L)]Cl_2$ complex showed four decomposition steps. The first decomposition step accompanied by loss of 2HCl and C_6H_5 molecules in the temperature range of 40-180 ºC with an estimated weight loss of 17.45% (calcd. 17.31%). The second decomposition step was accompanied by loss of 3NO and $C_{14}H_{19}N_2O$. molecules in the temperature range of 180-400 ºC with an estimated weight loss of 31.34% (calcd. 31.52%). The third and fourth steps of decomposition showed loss of $C_{18}H_{17}NO_2$ and $C_{12}H_9O$. molecules at 400-600 ºC and 600-1000 ºC with an estimated weight loss of 27.00% (calcd. 27.46%) and 16.29% (calcd. 15.9). Thereafter, the percentage of the residue corresponds to zinc oxide contaminated with carbon and the total approximate weight loss was found to be 92.08% (calcd. 92.19%).

The TG thermogram of $[Mn(H_2L)]Cl_2$ complex showed four decomposition steps. The first decomposition step accompanied by loss of 2HCl and C_2H_4 molecules in the temperature range of 50-270 ºC with an estimated weight loss of 14.23% (calcd. 13.97%). The second decomposition step accompanied by loss of $3N_2O$ and C_2H_2 molecules in the temperature range of 270-520 ºC with an estimated weight loss of 15.98% (calcd. 15.64%).

The third and fourth steps of decomposition showed loss of $C_{35}H_{20}O_3$ and $C_{10}H_{22}O$ molecules at 520-750 ºC and 750-1000 ºC with an estimated weight loss of 47.56% (calcd. 48.20%) and 15.39% (calcd. 15.27%). Thereafter, the percentage of the residue corresponds to manganese oxide contaminated with carbon and the total approximate weight loss was found to be 93.16% (calcd. 93.08%).

3.9. Structura1 interpretation

According to the analytical and spectroscopic data previously described, the

Proposed structures of metal complexes were given in Figure 4.

Table 2. Thermoanalytical results (TG, DTG and DTA) for Schiff base ligand and metal complexes

Compound	TG range (°C)	DTG_{max} (°C)	n*	Mass Loss Total mass Loss Calcd (Estim) %	Assignment	Residue
H_2L	25–270 270–520 520-770 770-1000	200 400 650 820	1 1 1	15.38 (15.35) 27.56 (27.36) 37.23 (36.95) 98.78 (99.75) 18.61 (20.09)	- Loss of N_2O and C_7H_7 - Loss of 4NO and C_9H_9 -Loss of $C_{22}H_{24}O_2$ -Loss of $C_{12}H_{14}O$	--------
$[Cd(H_2L)(H_2O)_2]Cl_2$	60-150 150-370 370-550 550-780 780-1000	100 250 440 670 ٩٢٠	1 1 ١ ١ ١	8.36 (8.07) 20.25 (20.75) 28.41 (28.22) 18.75 (18.45) 85.33 (84.91) 9.56 (9.42)	- Loss of 2HCL and CH_4. - Loss of 3NO and C_9H_9N. - Loss of N_2O and $C_{20}H_{12}$. - Loss of $C_{13}H_{12}O_2$. - Loss of $C_7H_{13}O$	CdO
$[Zn(H_2L)(H_2O)_2]Cl_2$	40-180 180-400 400-600 600-1000	120 250 500 800	1 1 ١ ١	17.31 (17.45) 31.52 (31.34) 27.46 (27.00) 92.19 (92.08) 15.9 (16.29)	- Loss of 2HCL and C_6H_5. - Loss of 3NO and $C_{14}H_{19}N_2O$. - Loss of $C_{18}H_{17}NO_2$. - Loss of $C_{12}H_9O$.	ZnO
$[Mn(H_2L)]Cl_2$	50-280 280-520 520-780 780-1000	200 350 650 850	1 1 ١ ١	13.97 (14.23) 15.64 (15.98) 48.20 (47.56) 93.08 93.16) 15.27 (15.39)	- Loss of HCl and $3CH_2$ - Loss of $3N_2O$ and C_2H_2 - Loss of $C_{35}H_{20}O_3$ - Loss of $C_{10}H_{22}O$	MnO

n* = number of decomposition steps.

3.10. Molecular Docking

Auto Dock is considered as one of the modern methods used to illustrate and demonstrate the benefits of biological features of Schiff bases and metal complexes and shed light on experimental data. Docking was applied for ligand (guest) with different kinds of organisms (various protein receptors) as host such as: Bacillus subtilis (5ZW4-A), Escherichia coli (3HUM-A), Pseudomonas aeruginosa (4WEL-A) and Staphylococcus aureus (5M18-A). Also, the energies for the docking procedure can be calculated. The strong interaction with all receptors with comparable results can be determined from HB plots (Figures 4–7) according to computation. Inter-hydrogen bonding was clearly visible for all proteins. The mode of interaction inside the docking molecules can be visualized by two-dimensional plots (Figures 4–7).

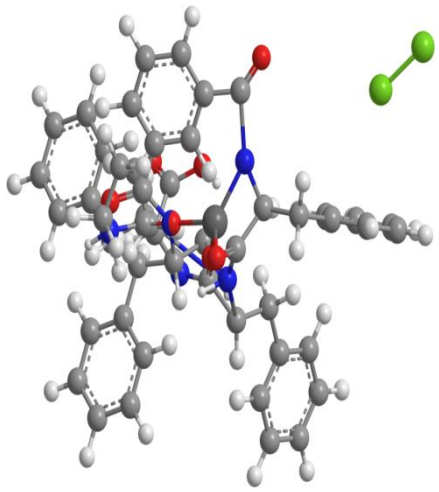

Figure 3 Structure of metal complexes of Schiff base ligand.

It appeared that the interaction occurred between the amino acids of proteins and the Schiff base ligand via hydrogen bonds as follows: Bacillus subtilis (5ZW4-A), Escherichia coli (3HUM-A), Pseudomonas aeruginosa (4WEL-A) and Staphylococcus aureus (5M18-A): amino acid of protein reacted with ligand by H-bond of Bacillus subtilis (5ZW4-A): 5zw4-pdb-H//A/ASP`133/O – with hydrogen bond length = 3.3 Å, 5zw4-pdb-H//A/GLY`62/O – with hydrogen bond length = 3.4 Å, 5zw4-pdb-H//A/ARG`90/2HH2– with hydrogen bond length = 1.5 Å, 5zw4-pdb-H//A/ALA`64/HN – with hydrogen bond length = 2.5 Å, 5zw4-pdb-H//A/GLU`85/OE1 – with hydrogen bond length = 2.3 Å, 5zw4-pdb-H//A/ARG`86/2HH1`A – with hydrogen bond length = 2.0 Å and 5zw4-pdb-H//A/ARG`86/2HH1`A – with hydrogen bond length = 2.7 Å, with binding energy = −7.5 kcal mol^{-1} (Figures 6–9).

For E. coli (3HUM-A): the amino acids of protein reacted with ligand by H-bond as follow: 3HUM-A A/TYR`291/OH –with hydrogen bond length = 2.5 Å, 3HUM -A/TYR`268/OH – with hydrogen bond length = 3.3 Å, 3HUM -A/GLU`297/OE1– with hydrogen bond length = 3.1 Å, 3HUM -A/GLU`297/OE1– with hydrogen bond length = 2.3 Å, 3HUM -A/CEW`501/O17– with hydrogen bond length = 2.8 Å , 3HUM-CEW`501/N10– with hydrogen bond length = 3.5 Å , 3HUM -A/LEU`115/O – with hydrogen bond length = 2.1 Å, 3HUM -A/LEU`112/CG – with hydrogen bond length = 3.6 Å, 3HUM -A/THR`118/N – with hydrogen bond length = 3.4 Å, 3HUM -A/ASN`138/OD1– with hydrogen bond length = 3.1 Å, 3HUM -A/ILE`134/CD1– with hydrogen bond length = 3.3 Å, 3HUM -A/VAL`100/CG2– with hydrogen bond length = 3.3 Å and 3HUM -A/TYR`238/OH – with hydrogen bond length = 2.9 Å, with binding energy = − 8 kcal mol^{-1}.

For P. aeruginosa (4wel): amino acid of protein reacts with ligand by H-bond: 4wel-A/ASP`515/OD2– with hydrogen bond length = 3.6 Å, 4wel-A/ASP`428/OD2– with hydrogen bond length = 2.7 Å, 4wel-A/GLN`447/NE2– with hydrogen bond length = 3.2 Å, 4wel-A/LYS`430/NZ – with hydrogen bond length = 3.4 Å, 4wel-A/ALA`481/N –with hydrogen bond length = 3.4 Å and 4wel-A/VAL`388/CG2–with hydrogen bond length = 1.7 Å, with binding energy = −4.4 kcal mol^{-1}.

For S. aureus (5M18-A): amino acid of protein reacted with ligand by H- bond: 5M18- A /A/GLU`170/OE1 –with hydrogen bond length = 2.5 Å, 5M18- A /A/LYS`148/NZ –with hydrogen bond length = 3.2 Å, 5M18-A /A/THR`238/OG1 = 3.4 Å, 5M18-A / A/GLU`239/OE2–with hydrogen bond length = 2.5 Å, 5M18-A / A/GLU`239/OE2–with hydrogen bond length = 3 Å, 5M18-A / A/MUR`703/O6–with hydrogen bond length = 1.1 Å, 5M18-A / A/THR`165/CG2–with hydrogen bond length = 2.1 Å, 5M18-A - A/ASP`274/OD1–with hydrogen bond length = 2.3 Å, 5M18-A / A/MUR`703/O4–with hydrogen bond length = 3.6 Å, 5M18-A / A/THR`165/OG1–with hydrogen bond length = 2.6 Å, 5M18-A / A/MUR`703/O1–with hydrogen bond length = 0.8 Å, 5M18-A / A/ARG`241/N –with hydrogen bond length = 3.2 Å, 5M18-A / A/SER`240/OG –with hydrogen bond length = 2.5 Å, 5M18-A / A/GLY`166/O –with hydrogen bond length = 1.6 Å and 5M18-A / A/GLU`239/O –with hydrogen bond length = 3.3 Å, with binding energy = − 9.2 kcal mol^{-1} (Figures 4–7)

3.11. Antimicrobial activity

Schiff bases are an important class of compounds as they have wide range of applications in the medicinal field. They display biological activities as antibacterial [56, 57] and antitumor activities. Microbes are exposed to or confronted with a variety of different metal ions in the surrounding environment, which in turn interact with them, and are often useful to humans and sometimes others are more dangerous and damaging. The benefit and damage depend on their nature, whether chemical or physical, and also on the state of oxidation of the metal ion.

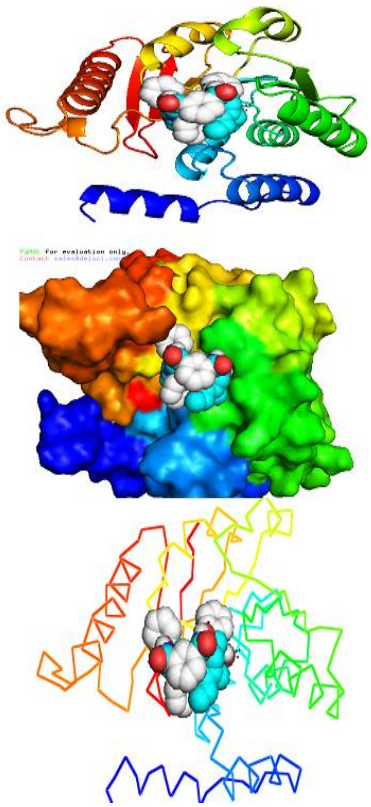

Figure 4. Three-dimensional plot of interaction of Schiff base ligand with (3HUM-A)E. coli receptor.

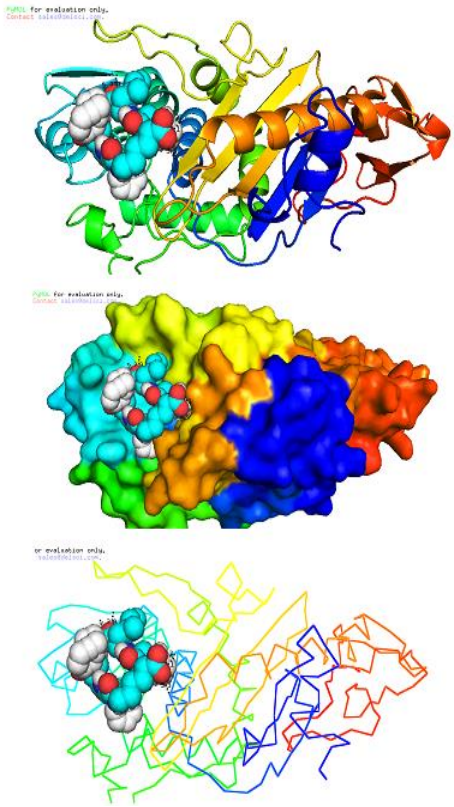

Figure 5. Three-dimensional plot of interaction of Schiff base ligand with (5M18-A). aureus receptor

It is very necessary to study the presence of these ions and how to find them, and it is observed that they are often found as cations (or cationic compounds) or oxy anions, such as salts or oxides in crystalline form or insoluble deposits in an insoluble form. From the study of these microbes, it is found that they have a great ability to overlap and bind the metal ions in the external environment on the surface of cells and transferred to the cell for different functions within the cells. All microbes, whether eukaryotic or eukaryotic, use metals for structural and/or catalytic functions. Antimicrobial activity was determined for the Schiff base and its complexes using the diffusion agar method [57]. Streptomycin was considered as a reference biochemical antibiotic for antibacterial activities. In examining the antibacterial activity of these complexes, more than one organism is used to increase the chance of detecting antibiotic activities in the test materials. Gram-positive (*S. aureus* ATTC12600 and *B. subtilis* ATTC 6051) and Gram-negative (*P. aeruginosa* ATTC 13315 and *E. coli* ATTC 11775) bacteria were used as test organisms. The antibacterial behavior was estimated by evaluating the inhibition zone diameter (mm) and minimum inhibitory concentration (MIC_{50}) (Figure 8).

It was observed that the Schiff base ligand has less activity towards Gram-positive and toward Gram-negative bacteria as can see from Figure (8). The activity of Zn(II) complex is higher than Cd(II) complex than ligand towards *B. subtilis*, *S. aureus*, *E. coli* and *P. aeruginosa* organisms with inhibition zone values of 14, 20, 14 and 16 mm/mg, respectively, for Zn(II) complex and inhibition zone values of 23, 26, 21 and 24 mm/mg, respectively, for Cd(II) complex. Whereas Mn(II) complex has no effect towards *B. subtilis*, *S. aureus*, *E. coli* and *P. aeruginosa* organisms.

4. Conclusion

In order to classify the Schiff base ligand under investigation and its transition metal complexes, various physicochemical, spectroscopic and thermal methods of analysis were used. In addition, the $[Zn(H_2L)]Cl_2$ complex was classified as the most active antibacterial/antifungal compound among them when researching their antimicrobial activities. Docking studies of ligand was studied, giving that variation of activity of ligand towards different types of proteins with minimum binding energy that can interact with several receptors in the proteins studied.

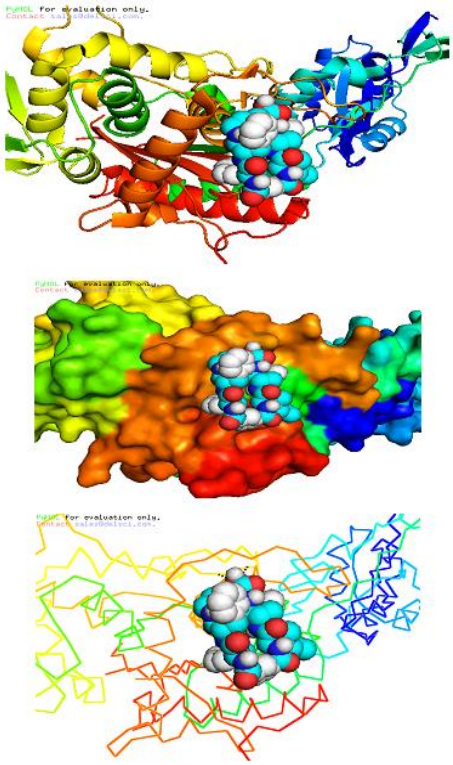

Figure 6. Three-dimensional plot of interaction of Schiff base ligand with (5ZW4-A) B. subtilis receptor

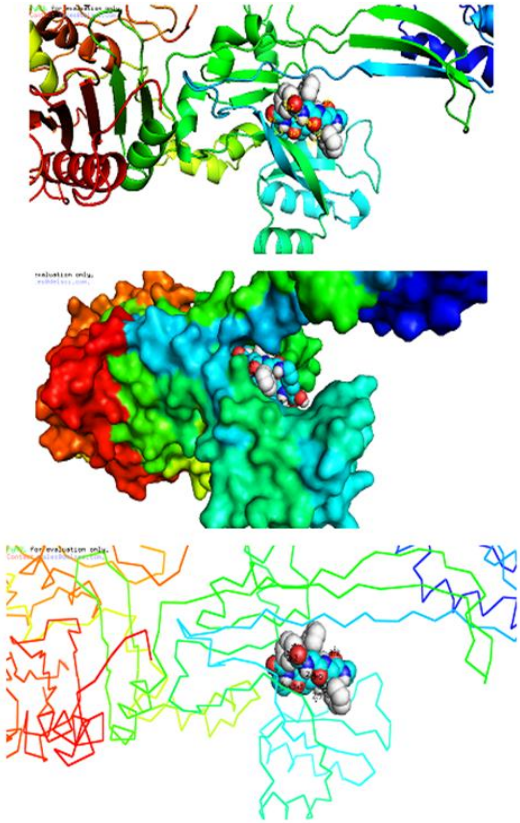

Figure 7. Three-dimensional plot of interaction of Schiff base ligand with (4we)l P. aeruginosa receptor

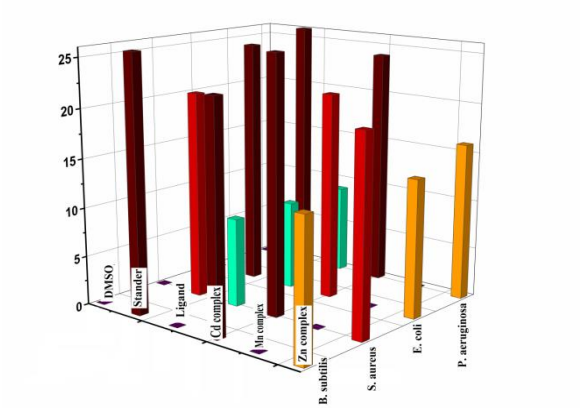

Figure 8. Biological activity of Schiff base ligand and its metal complexes.

References

[1] J. Jumina, R.E. Sarjono, D. Siswanta, S.J. Santosa, K. Ohto, Adsorption characteristics of Pb (II) and Cr (III) onto C-Methylcalix [4] resorcinarene, Journal of the Korean Chemical Society 55(3) (2011) 454-462.

[2] S.N. Lopez, M.V. Castelli, S.A. Zacchino, J.N. Domínguez, G. Lobo, J. Charris-Charris, J.C. Cortés, J.C. Ribas, C. Devia, A.M. Rodríguez, In vitro antifungal evaluation and structure–activity relationships of a new series of chalcone derivatives and synthetic analogues, with inhibitory properties against polymers of the fungal cell wall, Bioorganic & medicinal chemistry 9(8) (2001) 1999-2013.

[3] R.M. Mohareb, M.Y. Zaki, N.S. Abbas, Synthesis, anti-inflammatory and anti-ulcer evaluations of thiazole, thiophene, pyridine and pyran derivatives derived from androstenedione, Steroids 98 (2015) 80-91.

[4] O.J. Mohammed, M.F. Radi, A. Abdula, B. Al-Ahdami, W. Rodhan, H. Sha'aban, Synthesis of four chalcone derivatives bearing heterocyclic moieties as new Ache inhibitors by docking simulation, Int. J. Chem. Sci 13(1) (2015) 157-166.

[5] M.I. Alkhalaf, Attenuating effect of Indole-3-Carbinol on gold nanoparticle induced hepatotoxicity in rats, Arabian Journal of Chemistry 13(11) (2020) 8060-8068.

[6] M. Diab, G.G. Mohamed, W. Mahmoud, A. El-Sonbati, S.M. Morgan, S. Abbas, Inner metal complexes of tetradentate Schiff base: Synthesis, characterization, biological activity and molecular docking studies, Applied Organometallic Chemistry 33(7) (2019) e4945.

[7] A. Palanimurugan, A. Kulandaisamy, DNA, in vitro antimicrobial/anticancer activities and biocidal based statistical analysis of Schiff base metal complexes derived from salicylalidene-4-imino-2, 3-dimethyl-1-phenyl-3-pyrazolin-5-one and 2-aminothiazole, Journal of organometallic chemistry 861 (2018) 263-274.

[8] T. Thirunavukkarasu, H.A. Sparkes, K. Natarajan, V. Gnanasoundari, Synthesis, characterization and biological studies of a novel Cu (II) Schiff base complex, Inorganica Chimica Acta 473 (2018) 255-262.

[9] B. Iftikhar, K. Javed, M.S.U. Khan, Z. Akhter, B. Mirza, V. Mckee, Synthesis, characterization and biological assay of Salicylaldehyde Schiff base Cu (II) complexes and their precursors, Journal of Molecular Structure 1155 (2018) 337-348.

[10] D.K. Mahapatra, S.K. Bharti, V. Asati, Anti-cancer chalcones: Structural and molecular target perspectives, European journal of medicinal chemistry 98 (2015) 69-114.

[11] C. Karthikeyan, N. SH Narayana Moorthy, S. Ramasamy, U. Vanam, E. Manivannan, D. Karunagaran, P. Trivedi, Advances in chalcones with anticancer activities, Recent patents on anti-cancer drug discovery 10(1) (2015) 97-115.

[12] M. Ritter, R. Mastelari Martins, D. Dias, C. MP Pereira, Recent advances on the synthesis of chalcones with antimicrobial activities: a brief review, Letters in Organic Chemistry 11(7) (2014) 498-508.

[13] A. Budhiraja, K. Kadian, M. Kaur, V. Aggarwal, A. Garg, S. Sapra, K. Nepali, O. Suri, K. Dhar, Synthesis and biological evaluation of naphthalene, furan and pyrrole based chalcones as cytotoxic and antimicrobial agents, Medicinal Chemistry Research 21(9) (2012) 2133-2140.

[14] Z. Nowakowska, A review of anti-infective and anti-inflammatory chalcones, European journal of medicinal chemistry 42(2) (2007) 125-137.

[15] Y.-H. Wang, H.-H. Dong, F. Zhao, J. Wang, F. Yan, Y.-Y. Jiang, Y.-S. Jin, The synthesis and synergistic antifungal effects of chalcones against drug resistant Candida albicans, Bioorganic & medicinal chemistry letters 26(13) (2016) 3098-3102.

[16] K.V. Sashidhara, K.B. Rao, P. Kushwaha, R.K. Modukuri, P. Singh, I. Soni, P. Shukla, S. Chopra, M. Pasupuleti, Novel chalcone–thiazole hybrids as potent inhibitors of drug resistant Staphylococcus aureus, ACS medicinal chemistry letters 6(7) (2015) 809-813.

[17] C. Zhuang, W. Zhang, C. Sheng, W. Zhang, C. Xing, Z. Miao, Chalcone: a privileged structure in medicinal chemistry, Chemical reviews 117(12) (2017) 7762-7810.

[18] D. D Jandial, C. A Blair, S. Zhang, L. S Krill, Y.-B. Zhang, X. Zi, Molecular targeted approaches to cancer therapy and prevention using chalcones, Current cancer drug targets 14(2) (2014) 181-200.

[19] R. Sharma, R. Kumar, R. Kodwani, S. Kapoor, A. Khare, R. Bansal, S. Khurana, S. Singh, J. Thomas, B. Roy, A review on mechanisms of anti tumor activity of chalcones, Anti-Cancer Agents in Medicinal Chemistry (Formerly Current Medicinal Chemistry-Anti-Cancer Agents) 16(2) (2016) 200-211.

[20] N. K Sahu, S. S Balbhadra, J. Choudhary, D. V Kohli, Exploring pharmacological significance of chalcone scaffold: a review, Current medicinal chemistry 19(2) (2012) 209-225.

[21] A.M. Naglah, G.O. Moustafa, A.A. Elhenawy, M.M. Mounier, H. El-Sayed, M.A. Al-Omar, A.A. Almehizia, M.A. Bhat, Nα-1, 3-Benzenedicarbonyl-Bis-(Amino Acid) and Dipeptide Candidates: Synthesis, Cytotoxic, Antimicrobial and Molecular Docking Investigation, Drug Design, Development and Therapy 15 (2021) 1315.

[22] E.M. Zayed, M.A. Zayed, H.A. Abd El Salam, G.A. Nawwar, Synthesis, structural characterization, density functional theory (B3LYP) calculations, thermal behaviour, docking and antimicrobial activity of 4-amino-5-(heptadec-8-en-1-yl)-4H-1, 2, 4-triazole-3-thiol and its metal chelates, Applied Organometallic Chemistry 32(12) (2018) e4535.

[23] E.M. Zayed, M.A. Zayed, A.M. Fahim, F.A. El-Samahy, Synthesis of novel macrocyclic Schiff's-base and its complexes having N2O2 group of donor atoms. Characterization and anticancer screening are studied, Applied Organometallic Chemistry 31(9) (2017) e3694.

[24] A.R. Chacko, J. Jeyakanthan, G. Ueno, K. Sekar, C.D. Rao, E.J. Dodson, K. Suguna, R.J. Read, A new pentameric structure of rotavirus NSP4 revealed by molecular replacement, Acta Crystallographica Section D: Biological Crystallography 68(1) (2012) 57-61.

[25] E.M. Zayed, F.A. El-Samahy, G.G. Mohamed, Structural, spectroscopic, molecular docking, thermal and DFT studies on metal complexes of bidentate orthoquinone ligand, Applied Organometallic Chemistry 33(9) (2019) e5065.

[26] M.G. Dekamin, Z. Karimi, Z. Latifidoost, S. Ilkhanizadeh, H. Daemi, M.R. Naimi-Jamal, M. Barikani, Alginic acid: A mild and renewable bifunctional heterogeneous biopolymeric organocatalyst for efficient and facile synthesis of polyhydroquinolines, International journal of biological macromolecules 108 (2018) 1273-1280.

[27] K.M. Khan, M.T. Muhammad, I. Khan, S. Perveen, W. Voelter, Rapid cesium fluoride-catalyzed Knoevenagel condensation for the synthesis of highly functionalized 4, 4′-(arylmethylene) bis (1 H-pyrazol-5-ol) derivatives, Monatshefte für Chemie-Chemical Monthly 146(9) (2015) 1587-1590.

[28] P.R. Schauer, D.L. Bhatt, J.P. Kirwan, K. Wolski, A. Aminian, S.A. Brethauer, S.D. Navaneethan, R.P. Singh, C.E. Pothier, S.E. Nissen, Bariatric surgery versus intensive medical therapy for diabetes—5-year outcomes, N Engl J Med 376 (2017) 641-651.

[29] E.M. Zayed, M. Zayed, H.A. Abd El Salam, M.A. Noamaan, Novel Triazole Thiole ligand and some of

its metal chelates: Synthesis, structure charactertization, thermal behavior in comparison withcomputational caculations andbiological activities, Computational biology and chemistry 78 (2019) 260-272.

[30] E.M. Zayed, M. Zayed, Synthesis of novel Schiff's bases of highly potential biological activities and their structure investigation, Spectrochimica Acta Part A: Molecular and Biomolecular Spectroscopy 143 (2015) 81-90.

[31] I. Borges, J. Danielli, V. Silva, L. Sallum, J. Queiroz, L. Dias, I. Iermak, G. Aquino, A. Camargo, C. Valverde, Synthesis and structural studies on (E)-3-(2, 6-difluorophenyl)-1-(4-fluorophenyl) prop-2-en-1-one: a promising nonlinear optical material, RSC Advances 10(38) (2020) 22542-22555.

[32] J. Jumina, R.W. Styaningrum, D. Siswanta, S. Triono, Y. Priastomo, H. Harizal, E.N. Sholikhah, A.K. Zulkarnain, Synthesis and preliminary evaluation of several chalcone derivatives as sunscreen compounds, Chemistry Journal of Moldova 14(2) (2019) 90-96.

[33] W.M. Hassan, E.M. Zayed, A.K. Elkholy, H. Moustafa, G.G. Mohamed, Spectroscopic and density functional theory investigation of novel Schiff base complexes, Spectrochimica Acta Part A: Molecular and Biomolecular Spectroscopy 103 (2013) 378-387.

[34] E.M. Zayed, G.G. Mohamed, A.M. Hindy, Transition metal complexes of novel Schiff base, Journal of Thermal Analysis and Calorimetry 120(1) (2015) 893-903.

[35] Y. Kim, K. Hyun, D. Ahn, R. Kim, M.H. Park, Y. Kim, Efficient aluminum catalysts for the chemical conversion of CO2 into cyclic carbonates at room temperature and atmospheric CO2 pressure, ChemSusChem 12(18) (2019) 4211-4220.

[36] M.H. Ahmed, M.A. El-Hashash, M.I. Marzouk, A.M. El-Naggar, Design, synthesis, and biological evaluation of novel pyrazole, oxazole, and pyridine derivatives as potential anticancer agents using mixed chalcone, Journal of Heterocyclic Chemistry 56(1) (2019) 114-123.

[37] S. Ding, Z. Ni, M. Hu, G. Qiu, J. Li, J. Ye, X. Zhang, F. Liu, H. Dong, W. Hu, An Asymmetric Furan/Thieno [3, 2-b] Thiophene Diketopyrrolopyrrole Building Block for Annealing-Free Green-Solvent Processable Organic Thin-Film Transistors, Macromolecular rapid communications 39(15) (2018) 1800225.

[38] E.M. Zayed, G.G. Mohamed, W.M. Hassan, A.K. Elkholy, H. Moustafa, Spectroscopic, thermal, biological activity, molecular docking and density functional theoretical investigation of novel bis Schiff base complexes, Applied Organometallic Chemistry 32(7) (2018) e4375.

[39] E.M. Zayed, M. Zayed, A.M. Hindy, Thermal and spectroscopic investigation of novel Schiff base, its metal complexes, and their biological activities, Journal of Thermal Analysis and Calorimetry 116(1) (2014) 391-400.

[40] M.A. Gouda, M.A. Berghot, G.E. Abd El-Ghani, A.E.G.M. Khalil, Synthesis of Some Novel 4-(Furan-2-yl)-5, 6-dimethylpyridines, Journal of Heterocyclic Chemistry 55(8) (2018) 1935-1941.

[41] A.A. Shanty, P.V. Mohanan, Heterocyclic Schiff bases as non toxic antioxidants: Solvent effect, structure activity relationship and mechanism of action, Spectrochimica Acta Part A: Molecular and Biomolecular Spectroscopy 192 (2018) 181-187.

[42] M.S. Mohamed, A.O. Abdelhamid, F.M. Almutairi, A.G. Ali, M.K. Bishr, Induction of apoptosis by pyrazolo [3, 4-d] pyridazine derivative in lung cancer cells via disruption of Bcl-2/Bax expression balance, Bioorganic & medicinal chemistry 26(3) (2018) 623-629.

[43] E.M. Zayed, A.M. Hindy, G.G. Mohamed, Molecular structure, molecular docking, thermal, spectroscopic and biological activity studies of bis-Schiff base ligand and its metal complexes, Applied Organometallic Chemistry 32(1) (2018) e3952.

[44] B. Vijayakumar, V. Kannappan, V. Sathyanarayanamoorthi, DFT analysis and spectral characteristics of Celecoxib a potent COX-2 inhibitor, Journal of Molecular Structure 1121 (2016) 16-25.

[45] W.H. Mahmoud, R.G. Deghadi, G.G. Mohamed, Novel Schiff base ligand and its metal complexes with some transition elements. Synthesis, spectroscopic, thermal analysis, antimicrobial and in vitro anticancer activity, Applied Organometallic Chemistry 30(4) (2016) 221-230.

[46] M. Khajehzadeh, M. Moghadam, Molecular structure, FT IR, NMR, UV, NBO and HOMO–LUMO of 1-(3-(dimethylamino) propyl)-1-(4-fluorophenyl)-1, 3-dihydroisobenzofuran-5-carbonitrile by DFT/B3LYP and PBEPBE methods with LanL2DZ and 6-311++ G (d, 2p) basis sets, Spectrochimica Acta Part A: Molecular and Biomolecular Spectroscopy 180 (2017) 51-66.

[47] S. Andotra, S. Kumar, M. Kour, V. Sharma, S. Jaglan, S.K. Pandey, Synthesis, spectroscopic, DFT and in vitro biological studies of vanadium (III) complexes of aryldithiocarbonates, Spectrochimica Acta Part A: Molecular and Biomolecular Spectroscopy 180 (2017) 127-137.

[48] M.A. Gouda, M.A. Berghot, G.E. Abd El-Ghani, A.E.-G.M. Khalilb, Month 2018 Synthesis of Some Novel 4-(Furan-2-yl)-5, 6-dimethylpyridines, (2018).

[49] F.M. Wang, D. Bao, M. Wang, Q.H. Yin, L.Z. Chen, G.F. Han, Synthesis of New 3-(Furan-2-yl)-Substituted Dibenzo-Diazepin-1-one Derivatives, Journal of Heterocyclic Chemistry 53(4) (2016) 1081-1085.

[50] P. Belanzoni, P. Carvalho, J. Theodoro, O. Thiemann, J. Ellena, H. Napolitano, DFT investigation on hydrogen bonding in cyclohexane-1, 2, 3, 4, 5-pentol crystal structure, Journal of Structural Chemistry 55(8) (2014) 1596-1606.

[51] V.S. Duarte, G.D. D'Oliveira, J.M. Custodio, S.S. Oliveira, C.N. Perez, H.B. Napolitano, Experimental and molecular modeling study of a novel arylsulfonamide chalcone, Journal of molecular modeling 25(7) (2019) 1-14.

[52] S. Pod, A. Mustafina, A. Koppehele, M. Grüner, W. Habicher, B. Buzykin, A. Konovalov, Synthesis of per-O-(carboxymethyl) calix [4] pyrogallols and their complexation with some alkaline metal and lanthanide ions, Russian chemical bulletin 53(6) (2004) 1181-1188.

[53] G.G. Mohamed, E.M. Zayed, A.M. Hindy, Coordination behavior of new bis Schiff base ligand derived from 2-furan carboxaldehyde and propane-1, 3-diamine. Spectroscopic, thermal, anticancer and antibacterial activity studies, Spectrochimica Acta Part A: Molecular and Biomolecular Spectroscopy 145 (2015) 76-84.

[54] Y. Xue, Y. Liu, L. Zhang, H. Wang, Q. Luo, R. Chen, Y. Liu, Y. Li, Antioxidant and spectral properties of chalcones and analogous aurones: theoretical insights, International Journal of Quantum Chemistry 119(3) (2019) e25808.

[55] C. Liu, A. Taheri, B. Lai, Y. Gu, Synergistic catalysis-induced ring-opening reactions of 2-substituted 3, 4-dihydropyrans with α-oxoketene dithioacetals, Catalysis Science & Technology 5(1) (2015) 234-245.

[56] R.F. Costa, A.S. Aguiar, I.D. Borges, R. Ternavisk, C. Valverde, A.J. Camargo, D. Braz, H.B. Napolitano, S.S. Oliveira, Effect of ortho-and para-chlorine substitution on hydroxychlorochalcone, Journal of Molecular Modeling 27(2) (2021) 1-22.

[57] J.F.A. Filho, N.A. Dos Santos, K.B. Borges, V. Lacerda Jr, F.S. Pelição, W. Romão, Fiber spray ionization mass spectrometry in forensic chemistry: A screening of drugs of abuse and direct determination of cocaine in urine, Rapid Communications in Mass Spectrometry 34 (2020) e8747.